RSC Advances

CrossMark
click for updates

p-Type doping of tetrafluorotetracynoquinodimethane (F$_4$TCNQ) in poly(*para*-phenylene vinylene) (PPV) derivative "Super Yellow" (SY)

Manisha Bajpai,*[ac] Ritu Srivastava,[b] Ravindra Dhar,[a] R. S. Tiwari[c] and Suresh Chand[b]

In this paper, we report a case of hole transport in tetrafluorotetracynoquinodimethane doped poly(*para*-phenylene vinylene) derivative "Super Yellow". The hole mobility of pristine and doped polymer thin films was determined by impedance spectroscopy. The increase in hole mobility upon doping was also verified by current density–voltage measurements. It was found to be increased by two orders of magnitude upon doping. The increase in hole mobility upon p-type doping was explained on the basis of extended Gaussian disorder model by measuring current density–voltage characteristics in the same devices. At low bias, *J–V* characteristics exhibit clear space charge limited conduction in pristine state but ohmic behaviour when doped. Further, at higher voltages the current density increases non-linearly due to the field-dependent mobility and carrier concentration by filling of tail states of highest occupied molecular orbital of the host material. The room temperature *J–V* characteristics were well described with the single value of free hole density at low fields. At higher fields it becomes field-dependent followed by a field enhancement factor γ.

Introduction

Organic semiconductors based devices are advantageous compared to inorganic semiconductors because of their high absorption coefficients because most organic dyes emit in the visible range, making them suitable for very thin organic photo detector (OPD)[1–4] and photovoltaic (OPV)[5] applications. Other than this, some of the fluorescent dyes show strong red shifts during emission as compared to absorption and this property makes them perfect for organic light emitting diodes (OLEDs)[6,7] with no absorption losses.

Organic semiconductor can be doped either by removing an electron from the highest occupied molecular orbital (HOMO) or by adding an electron to the lowest unoccupied molecular orbital (LUMO) to increase its conductivity.[8–10] Doping in organic semiconductor creates high charge carriers which move in an electric field. This movement of charge is responsible for electrical conductivity in organic semiconductors.

Doping of a polymer is different than that of inorganic semiconductor, in which elements with an excess or shortage of electrons are introduced. In polymers, both doping processes involve both oxidation and reduction.[11–14] The first method involves exposing a polymer to an oxidant, such as iodine or bromine, or reductant such as alkali metals.

The second is electrochemical doping in which a polymer-coated electrode is suspended in an electrolyte solution. The polymer is insoluble in the solution that contains separate counter and reference electrodes. By applying an electric potential difference between the electrodes, counter ions from the electrolyte are diffused into the polymer in the form of electron addition (n-doping) or removal (p-doping). One of the problems with organic semiconductors is that p-type material is more prevalent than n-type because electron rich n-type is unstable in the presence of oxygen. Organic semiconductors can only be useful for devices if both p-type and n-type are incorporated.

p-Type doping was realized by enhanced hole injection into matrix followed by the modification of the interfaces by Blom *et al.*[15] They gave a new approach to understanding the effect of doping in organic semiconductors. Because the conductivity of any material is the product of carrier mobility and the number of charge carriers, increase in conductivity upon doping would result from the simultaneous increase of carrier concentration and carrier mobility. Generally, carrier transport in semiconducting materials takes place *via* hopping between the Gaussian density of states (GDOS). Consequently, if we ignore carrier density dependence, it will lead to an underestimation of the hopping distance and the width of the density of states in these

[a]Soft Materials Research Laboratory, Centre of Material Sciences, Institute of Interdisciplinary Studies, University of Allahabad, Allahabad, 211002, India. E-mail: mansa83@gmail.com

[b]Physics for Energy Harvesting Division, National Physical Laboratory (Council of Scientific and Industrial Research), Dr K. S. Krishnan Road, New Delhi 110012, India

[c]Department of Physics, Banaras Hindu University, Varanasi-221005, India

polymers. Therefore, a density dependent mobility model in combination with electric field and temperature has been proposed.[16–18]

In this paper, we demonstrate the effect of p-type doping on the hole transport of Super Yellow (SY) in terms of carrier mobility and carrier density.

Experimental

For the hole transport study of SY polymer as a function of p-type doping, hole-only devices of SY polymer with different doping concentrations of F_4TCNQ were fabricated. SY and F_4TCNQ were dissolved in toluene under the concentrations of 6 mg ml^{-1} and 0.1 mg ml^{-1}, respectively. The solutions were stirred on a hot plate at 70 °C for 12 h and then filtered separately. Then SY and F_4TCNQ solutions were blended in different doping concentrations by a volumetric pipette under nitrogen atmosphere. 25 μL dimethyl sulfoxide (DMSO) was added into the solutions to prevent aggregation. Further, hole only devices in the configuration of ITO/SY:F_4TCNQ/Au were fabricated. The devices were prepared on ITO coated glass substrates (purchased from Vin Karola, USA; sheet resistance ∼18 Ω m^{-2}). Prior to use, the ITO coated glass substrates were cleaned by

deionized water, acetone, trichloroethylene and isopropyl alcohol for 20 min and finally dried in vacuum. Thereafter, the active layer was spin coated onto these cleaned glass substrates from solution at a spin speed of 1200 rpm resulting in a typical film thickness of 200 nm.

These films were then annealed at 150 °C in vacuum for 2 h. On top of these films, Au electrodes of 500 nm thickness were deposited by vacuum thermal evaporation at 5×10^{-6} Torr. The devices so obtained were sealed using UV irradiation on epoxy resin to inhibit atmospheric oxidation of electrodes. J–V characteristics of the pristine and doped samples in different temperature ranges were measured using a low temperature setup coupled with a Keithley 2400 Source Meter unit interfaced with a PC. A Solartron SI 1260 Impedance/Gain-Phase analyzer was used to measure the capacitance–frequency (C–f) spectra of the samples.

Results and discussion

In this work, we studied the effect of doping on the hole transport of Super Yellow (SY). The hole mobility of pristine and doped SY thin films was determined independently from
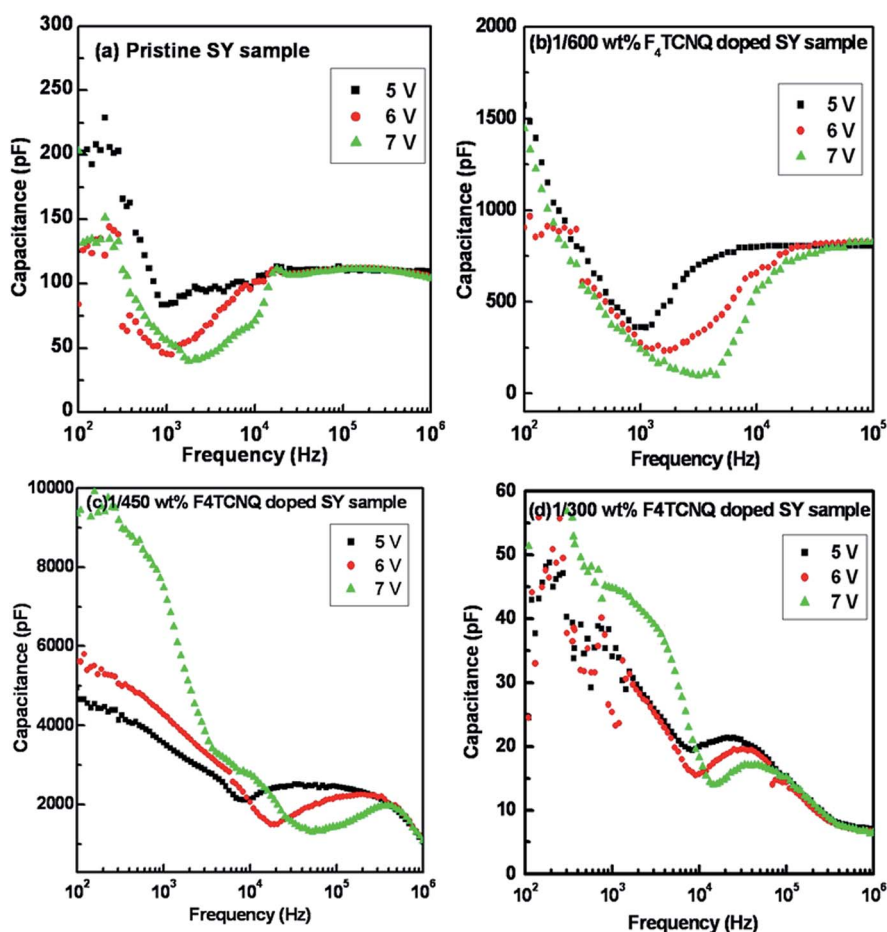

Fig. 1 Capacitances of (a) pristine, (b) 1/600 wt% F_4TCNQ doped, (c) 1/450 wt% F_4TCNQ doped and (d) 1/300 wt% F_4TCNQ doped hole only devices at room temperature.

impedance spectroscopy (IS)[19–22] by measuring frequency dependent capacitance spectra under varying applied biases.

We employed frequency dependent capacitance spectra for different applied d.c. biases ($V_{dc} = 5$, 6 and 7 volt) by measuring the a.c. signal of 100 mV over the frequency range 10 Hz to 10 MHz.

Fig. 1(a–d) shows the capacitance spectra of pristine and doped devices as a function of a.c. frequency (f) from 100 Hz to 1 MHz for the d.c. bias voltages of 5, 6 and 7 V. Bias voltage is essentially required to drift/hop charge carriers (holes), which is otherwise not possible under the small a.c. test voltage of 100 mV. At higher frequencies, a sharp cutoff appears in C–f spectra which approaches the vanishing point of the capacitance signal (see Fig. 1c). It is due to the reactive cutoff frequency of the structure. With increasing capacitance value, reactive cutoff frequency goes down.[22,23] Because the capacitance value is the highest in Fig. 1c, its reactive cutoff frequency is the lowest. With the increase in the bias voltage, the capacitance–frequency spectra changed drastically at transit frequency (f_t). This may be

due to the fact that the injected current lags behind the signal voltage due to the finite transit time (τ_{tr}). Therefore, the injection of additional space charge increases with applied voltage and these injected charge carriers will further move into the device to achieve new equilibrium space-charge distribution. Because of the finite τ_{tr}, the corresponding current lags behind the a.c. voltage, and this gives an inductive contribution to the capacitance. The amplitude of extremum point enhances and its position shifts towards higher frequencies with the increase of the bias voltage. This effect is more pronounced in doped samples as compared to pristine sample. At frequencies above the transit frequency, the period of applied a.c. field is too short to redistribute the space charge in the device. Hence, we used C–f spectra at the intermediate frequency range to extract the carrier mobility where transit time effect occurs.

We estimated the hole mobility of pristine and doped hole only device by using the susceptance method.[24–26] In this method, the peak in susceptance provides a definitive way for determining the transit time of the charge carriers in organic
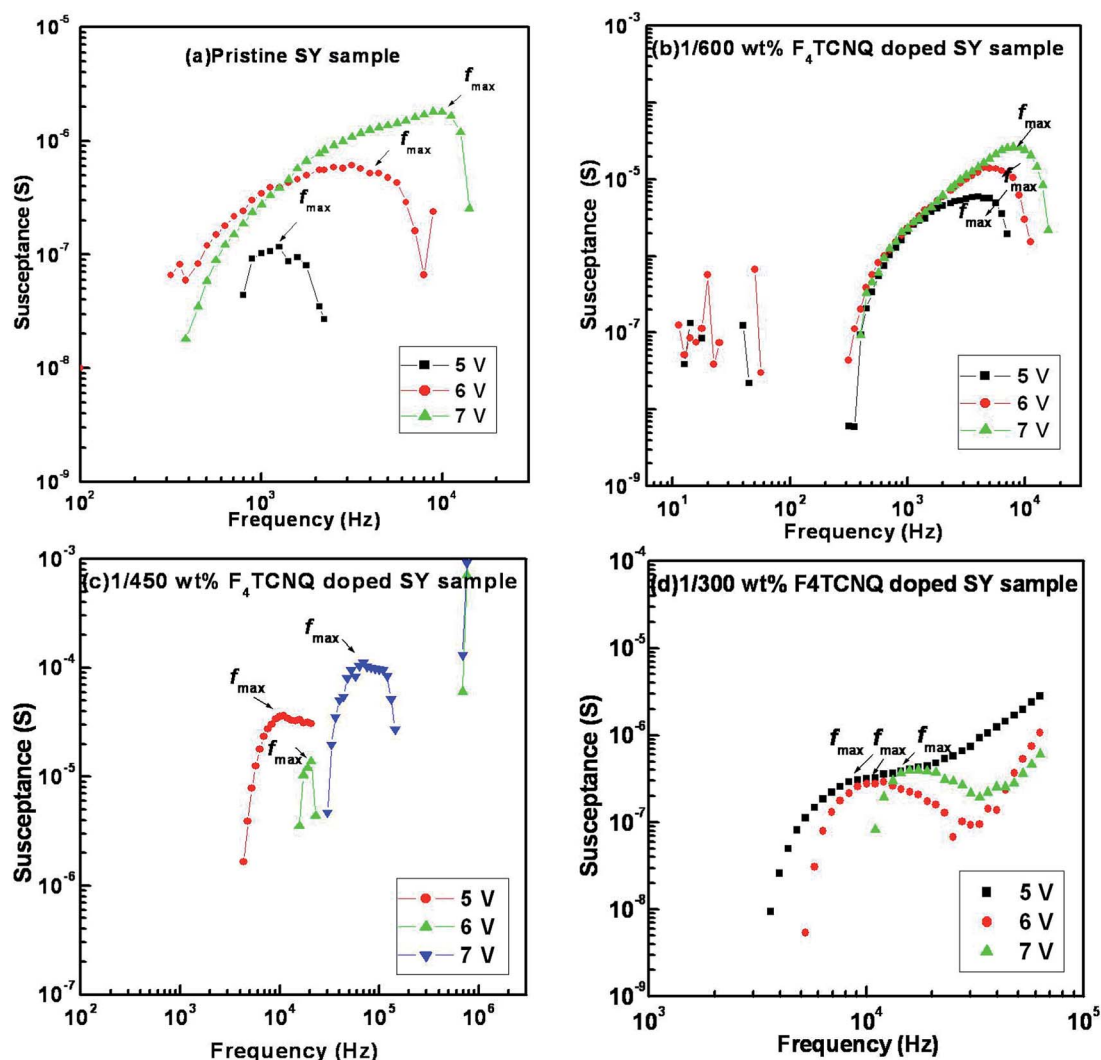

Fig. 2 Differential susceptance (ΔB) spectra at different bias voltages of (a) pristine, (b) 1/600 wt% F$_4$TCNQ doped, (c) 1/450 wt% F$_4$TCNQ doped and (d) 1/300 wt% F$_4$TCNQ doped hole only devices at room temperature.

materials corresponding to the frequency (f_{max}) where susceptance shows peak. As the voltage across the sample is changed, the f_{max} and hence the average transit time shifts enable the determination of mobility as a function of electric field. In this method, we extract the carrier transit time from susceptance plot, where negative differential susceptance is calculated as:

$$-\Delta B = \omega\{C(\omega) - C_0\} \quad (1)$$

where $\omega = 2\pi f$ is the angular frequency of the a.c. oscillations, $C(\omega)$ is the observed capacitance at a particular frequency and C_0 is geometrical capacitance of the organic layer ($C_0 = \varepsilon_0 A/L$, where ε_0 is the free space permittivity, A is the area of plates and L is the thickness of organic thin film).

The position of maximum of susceptance curves gives the transit time of hole (τ_{tr}) according to eqn (2).[27]

$$f_{max} = \frac{0.72}{\tau_{tr}} \quad (2)$$

In Fig. 2(a–d), we show the differential susceptance as function of the a.c. modulation frequency. The position and magnitude of the maximum of the ΔB curve are dependent on the bias voltage V_{dc}. When V_{dc} increases, the peak shifts towards high frequency region and its amplitude grows. Using the peak positions of the ΔB curves at different applied voltages, the hole mobility in pristine and doped SY films was determined using eqn (3).[28]

$$\mu_p = \frac{4}{3} \frac{d^2}{V_{dc}} \frac{1}{\tau_{tr}} \quad (3)$$

where μ is the hole mobility and d is the thickness of the polymer films. The hole mobility was calculated to be 2.58×10^{-8} cm^2 V^{-1} s^{-1} to 2.40×10^{-7} cm^2 V^{-1} s^{-1} for pristine SY thin films, 5.34×10^{-8} cm^2 V^{-1} s^{-1} to 1.28×10^{-7} cm^2 V^{-1} s^{-1} for 1 : 600 doped SY thin films, 3.21×10^{-7} cm^2 V^{-1} s^{-1} to 2.71×10^{-6} cm^2 V^{-1} s^{-1} for 1 : 450 doped SY thin films and 6.80×10^{-7} cm^2 V^{-1} s^{-1} to 1.00×10^{-6} cm^2 V^{-1} s^{-1} for 1 : 300 doped SY thin films for V_{dc} ranging from 5 to 7 volts. The mobility obtained in pristine sample is comparable to those measured by Bisquert *et al.* using the IS technique.[29] These results are further supported by the d.c. measurements on the samples described in the forthcoming paragraphs.

For the d.c. analysis, we measured *J–V* characteristics of pristine and doped SY samples at room temperature as well as elevated temperatures (230–290 K).

Fig. 3 shows the current density *versus* voltage (*J–V*) characteristics of SY hole only device with and without dopants at room temperature. At low bias voltages, the hole mobility (μ_p) is constant and the *J–V* characteristics follow the Child's law given by:[30]

$$J_{SCLC} = \frac{9}{8} \varepsilon_r \varepsilon_0 \mu_p \frac{V^2}{d^3} \quad (4)$$

where J_{SCLC} represent space charge limited current density. ε_r and ε_0 are the relative permittivity and free space permittivity respectively.
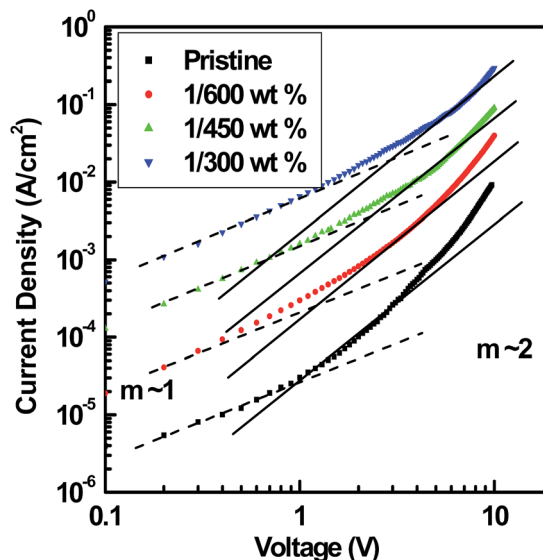

Fig. 3 Current density *versus* voltage characteristics of SY devices for different doping concentrations. The broken lines with slopes of 1 denote the ohmic current whereas the solid lines with slopes of 2 denote the space-limited current.

J–V characteristics at low voltages has a slope of 1, *i.e.* it shows ohmic conduction. It is requisite condition that metal–semiconductor interface must be an ohmic contact to achieve space charge limited (SCL) conduction. Therefore, to confirm the hole injection property ITO/SY interface, the measured (observed) current density (J_{obs}) was compared with the current density expected (J_{cal})[31] from trap free space charge limited of negatively charge p-dopants. The injection efficiency (η) is given as:

$$\eta = J_{obs}/J_{cal} \quad (5)$$

The calculated injection efficiency was found to be $\sim$−1 and therefore the formation of an ohmic contact with SY was confirmed. Hence, we can directly calculate hole mobility from *J–V* curves in the case of pristine as well as doped SY samples.

When F$_4$TCNQ is doped into polymer, free holes are generated into the polymer *via* p-type doping and these additional free holes are compensated by the negative charge of the corresponding acceptors. Therefore, doping induced free charge carriers will not contribute towards the space charge. Hence, in our calculations, we did not considered the effect of negatively charged p-dopants. Therefore, an ohmic-like current will flow at low voltages, given by:[32]

$$J_\Omega = qp_0\mu_p \frac{V}{d} \quad (6)$$

where p_0 is doping induced free hole density. Upon addition of p-type doping free holes are introduced into the organic semiconductor. At low voltages, p_0 will largely outnumber the charges that are injected from the contacts. Because p_0 is temperature-dependent due to a thermally

activated ionization process of the dopant, the mobility will not only depend on temperature but also on p_0, hence carrier density and mobility are included in eqn (6),[33] to give eqn (7):

$$J_\Omega(V, T) = qp_0(T)\mu_p(T, p_0(T), E)\frac{V}{d} \quad (7)$$

Further, to investigate the conduction mechanism in doped SY samples, the J–V characteristics were measured at various temperatures for doped SY devices with different doping ratios and are shown in Fig. 4(a–d). At low bias voltage the current density increases by 1–3 orders of magnitude with increasing doping concentrations. The solid lines with slope of 1 and 2 denote the ohmic and the space-limited current, respectively (it is already shown in Fig. 3 at room temperature, as doping concentration and field increases, more and more free charge carriers are generated and the ohmic-like current will flow

(already discussed in above section)). The J–V characteristics were numerically modelled using a recently developed transport model.[34] In this model, hole mobility depends on field E and hole density p. The hole mobility is given by:[34]

$$\mu_p(T, p, E) \approx \mu_p(T, p)f(T, E)$$
$$\mu_p(T, P) = \mu_0(T)\exp\left[\frac{1}{2}\left(\hat{\sigma}^2 - \hat{\sigma}\right)\left(2pa^3\right)^\delta\right]$$
$$f(T, E) = \exp\left\{0.44\left(\hat{\sigma}^{3/2} - 0.22\right)\left[\sqrt{1 + 0.8\left(\frac{Eea}{\sigma}\right)^2} - 1\right]\right\}$$
$$\delta = 2\frac{\ln\left(\hat{\sigma}^2 - \hat{\sigma}\right) - \ln(\ln 4)}{\hat{\sigma}^2}$$
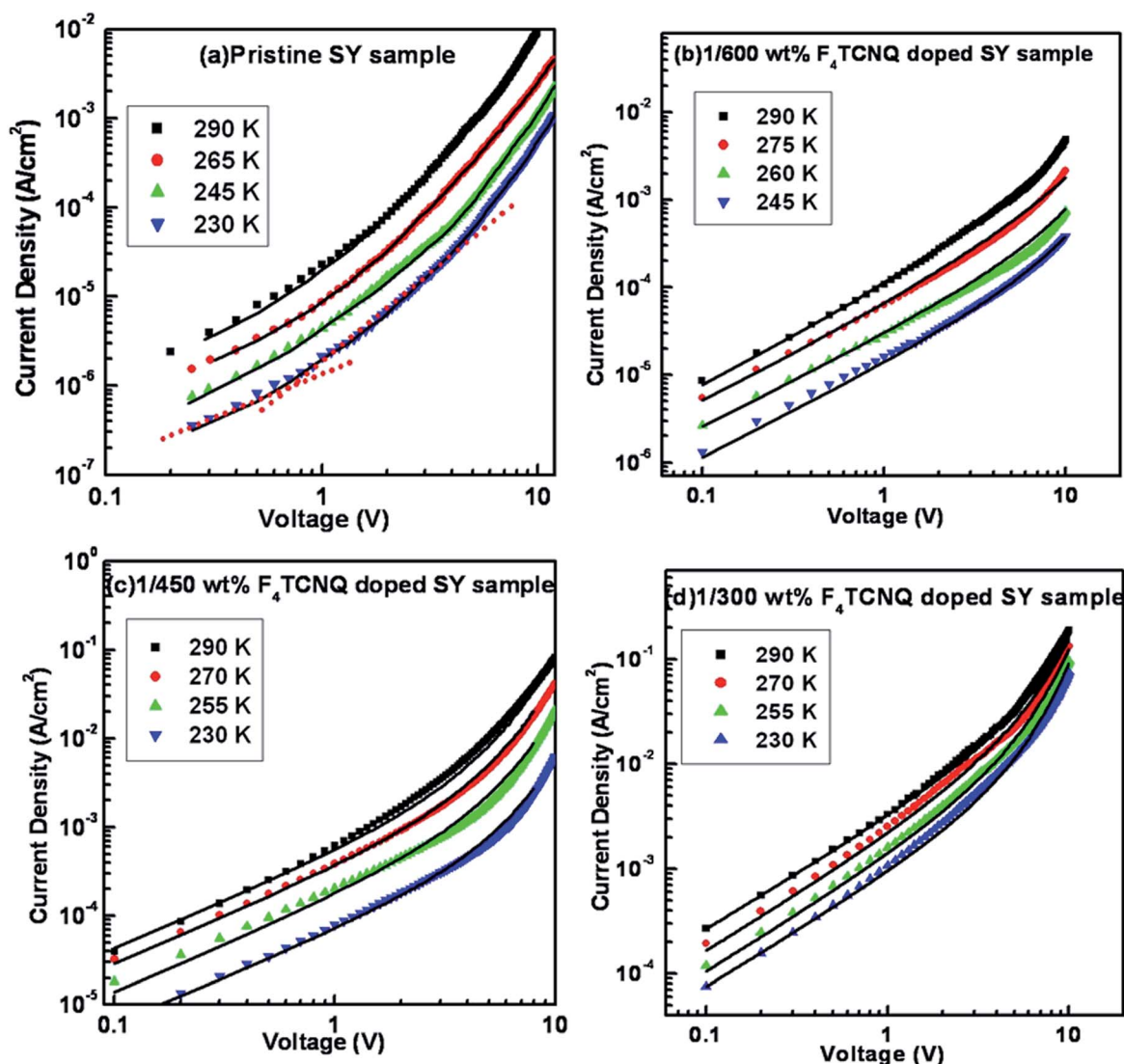$$\mu_0 = \frac{a^2 v_0 e}{\sigma} \quad (8)$$

Fig. 4 Temperature dependent current density *versus* voltage plot of (a) pristine, (b) 1/600 wt% F$_4$TCNQ doped, (c) 1/450 wt% F$_4$TCNQ doped and (d) 1/300 wt% F$_4$TCNQ doped hole only devices.

**Table 1** Comparison of calculated parameters from $J–V$ (space charge limited current) and susceptance method

	Hole mobility (cm^2 V^{-1} s^{-1})		
Samples	$J–V$ (SCLC) method	IS method at DC bias = 5 V	Disorder (meV)
Pristine	2.6×10^{-7}	2.58×10^{-8}	0.046
1 : 600	2.8×10^{-7}	5.34×10^{-8}	0.044
1 : 450	5.92×10^{-7}	3.21×10^{-7}	0.041
1 : 300	7.8×10^{-7}	6.80×10^{-7}	0.040

where $\hat{\sigma} = \sigma/K_B T$ and σ is the width of the Gaussian density of states, $a (= 1/N^{1/3})$ is the inter site distance (in our case, $a = 1.29$ nm for SY), and N is the density of transport sites. We found field-dependent mobility for pristine as well as doped SY samples as previously described in disordered materials in reports.[34] The fittings of the experimental $J–V$ curves with eqn (8) are shown by the solid lines in Fig. 4a–d and fitting parameters are listed in Table 1. In our calculations, we took a field-dependent $p_0(E)$ with a Poole–Frenkel like dependence on the applied electric field[35] The fittings of experimental $J–V$ curves is shown by the solid lines in Fig. 4a–d. These parameters fitted to $J–V$ curves for all devices and listed in Table 1. In our calculations, we have taken a field-dependent $p_0(E)$ with a Poole–Frenkel like dependence on the applied electric field[35]

$$p_0(E) = p_0(E = 0) \exp\left(\gamma\sqrt{E}\right) \tag{9}$$

where γ is the field-enhancement factor and $p_0(E = 0)$ is the zero field free hole density.

The field enhancement factor γ is the dependent on both electric field and temperature. Fig. 5 shows the electric field dependent hole density as a function of temperature. We found that hole density dependence on field is strongest in 1 : 450 wt% SY:F_4TCNQ doped sample as compared to other samples.
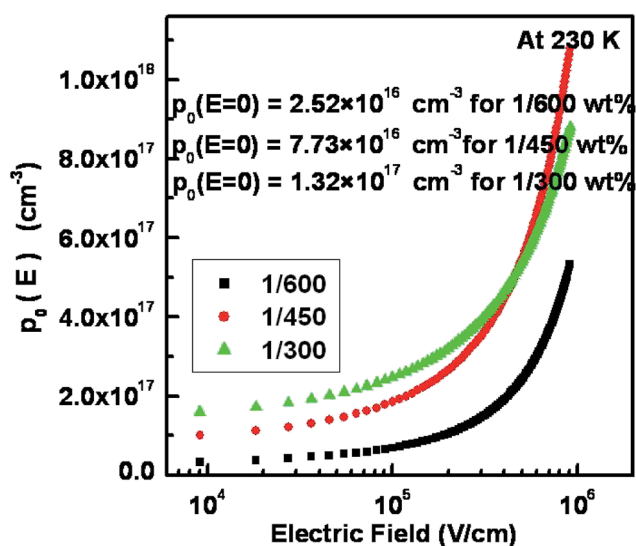
We observed similar effect with IS method as shown in Fig. 1. This result is attributed to the relatively low value of σ. Fig. 5 Electric field dependent free hole density ($p_0(E)$) at 230 K for 1 : 450% and 1 : 300% doped samples. For high doping concentrations, it is expected that the average distance that holes will have to hop from dopant to host will decrease.[36]

The calculated $J–V$ data for all the devices were found to fit in the above model and parameters obtained from simulation are summarized in Table 1. The increase or decrease in transport parameters upon doping can be qualitatively understood on the basis of a simple model based on disorder.

It is well known fact that in an organic semiconductor, HOMO has a Gaussian distribution. The density of states of pristine SY material is shown in Fig. 6. In disordered semi-conducting materials, the carrier transport usually occurs via hopping of charge carriers localized in the deep tail of GDOS. Charge carriers occupy only those states where the average distance between the charge carriers is large enough such that the transport of carrier is not affected by the presence of other carriers. This level is represented by $E_m = -\sigma^2/KT$. Thus carriers will hop from E_m to the next possible states. In organic materials, carrier transport is generally governed by SCL currents at low electric fields since there are fewer free carriers. At higher electric fields, background carrier concentration increases. Thus, carrier mobility is found to be electric field and density dependent. Further, in the case of F_4TCNQ doped SY material, obviously more carriers will be transferred to the lowest unoccupied molecular orbital (LUMO) of F_4TCNQ and therefore all F_4TCNQ molecules will be ionized. These ionized carriers will contribute to a doping induced free hole density by transferring the electrons from the tail states of GDOS and filled with holes. However, all these ionized carriers will not contribute in resulting the enhancement of carrier density. Only localized ionized F_4TCNQ carriers within the tail of HOMO of SY will produce the resulting enhancement.

Fig. 5 Electric field dependent free hole density ($p_0(E)$) at 230 K.
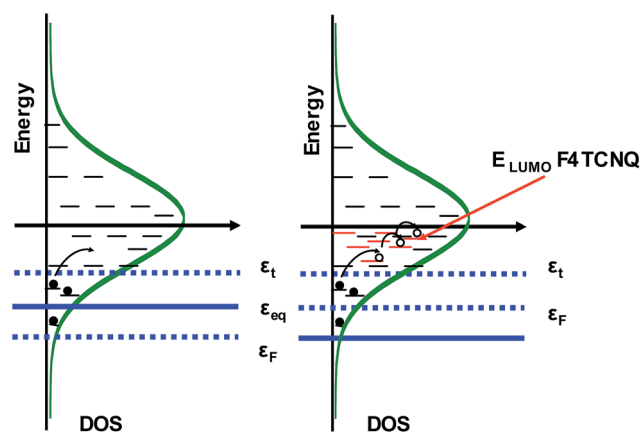
Fig. 6 Schematic representations of the density of states and the position of the Fermi level in (a) pristine SY sample and (b) in SY doped with F_4TCNQ. The red dashed line represents the LUMO level of F_4TCNQ.

Conclusions

We demonstrated the hole conduction mechanism in SY thin films as a function of doping. The charge carrier mobility of SY thin films was determined using impedance spectroscopy of the pristine and doped SY thin films. F_4TCNQ was used as a p-type dopant. The hole mobility was found to increase by 2 order of magnitude upon doping. It was observed that both mobility and carrier density increased with the doping of F_4TCNQ in SY. The dependence of the hole mobility on doping was explained by combining space-charge limited, field-effect and carrier density dependent measurements. It was inferred that free carriers are generated from acceptor molecules.

Acknowledgements

References

1 C. K. Chiang, C. R. Fincher Jr, Y. W. Park, A. J. Heeger, H. Shirakawa, E. J. Louis, S. C. Gau and A. G. MacDiarmid, *Phys. Rev. Lett.*, 1977, **39**, 1098.

2 M. Pfeiffer, A. Beyer, T. Fritz and K. Leo, *Appl. Phys. Lett.*, 1998, **73**, 3202.

3 W. Gao and A. Kahn, *Appl. Phys. Lett.*, 2001, **79**, 4040.

4 W. Gao and A. Kahn, *J. Appl. Phys.*, 2003, **94**, 359.

5 J. Blochwitz, T. Fritz, M. Pfeiffer, K. Leo, D. M. Alloway, P. A. Lee and N. R. Armstrong, *Org. Electron.*, 2001, **2**, 97.

6 W. Gao and A. Kahn, *J. Phys.: Condens. Matter*, 2003, **15**, 2757.

7 X. Zhou, J. Blochwitz, M. Pfeiffer, A. Nollau, T. Fritz and K. Leo, *Adv. Funct. Mater.*, 2001, **11**, 310.

8 J. Kido, K. Nagai and Y. Okamoto, *IEEE Trans. Electron Devices*, 1993, **40**, 1342.

9 J. Kido and T. Matsumoto, *Appl. Phys. Lett.*, 1998, **73**, 2866.

10 G. Werner, F. Li, K. Harada, M. Pfeiffer, T. Fritz and K. Leo, *Appl. Phys. Lett.*, 2003, **82**, 4495.

11 F. Li Werner, F. Li, K. Harada, M. Pfeiffer, T. Fritz, K. Leo and S. Machill, *Adv. Funct. Mater.*, 2004, **14**, 255.

12 F. Li, A. Werner, M. Pfeiffer, K. Leo and X. Liu, *J. Phys. Chem. B*, 2004, **108**, 17076.

13 M. Nollau, M. Pfeiffer, T. Fritz and K. Leo, *J. Appl. Phys.*, 2000, **87**, 4340.

14 K. Chan, F. Amy, Q. Zhang, S. Barlow, S. Marder and A. Kahn, *Chem. Phys. Lett.*, 2006, **431**, 67.

15 U. Zhang, B. de Boer and P. W. M. Blom, *Adv. Funct. Mater.*, 2009, **19**, 1901.

16 J. C. Blakesley, H. S. Clubb, N. C. Greenham and S. L. M. Van Mensfoort, *Phys. Rev. B: Condens. Matter Mater. Phys.*, 2010, **81**, 045210.

17 S. I. E. Vulto, R. A. J. Janssen and R. Coehoorn, *Phys. Rev. B: Condens. Matter Mater. Phys.*, 2008, **78**, 085208.

18 W. F. Pasveer, J. Cottaar, C. Tanase, R. Coehoorn, P. A. Bobbert, P. W. M. Blom, D. M. de Leeuw and M. A. J. Michels, *Phys. Rev. Lett.*, 2005, **94**, 206601.

19 B. Cobb, Y. T. Jeong and A. Dodabalapur, *Appl. Phys. Lett.*, 2008, **92**, 103302.

20 H. C. F. Martens, H. B. Brom and P. W. M. Blom, *Phys. Rev. B: Condens. Matter Mater. Phys.*, 1999, **60**, 8489.

21 H. C. F. Martens, J. N. Huiberts and P. W. M. Blom, *Appl. Phys. Lett.*, 2000, **77**, 1852.

22 R. Dhar, *Indian J. Pure Appl. Phys.*, 2004, **42**, 56.

23 T. Okachi, T. Nagase, T. Kobayashi and H. Naito, *Jpn. J. Appl. Phys.*, 2008, **47**, 8965.

24 D. C. Tripathi, A. K. Tripathi and Y. N. Mohapatra, *Appl. Phys. Lett.*, 2011, **98**, 033304.

25 N. D. Nguyen, M. Schmeits and H. P. Loebl, *Phys. Rev. B: Condens. Matter Mater. Phys.*, 2007, **75**, 075307.

26 H. Scher and E. W. Montroll, *Phys. Rev. B: Solid State*, 1975, **12**, 2455.

27 R. Kassing, *Phys. Status Solidi A*, 1975, **28**, 107.

28 J. M. Montero, J. Bisquert, G. G. Belmonte, H. J. Bolink and E. M. Barea, *Phys. Status Solidi A*, 2007, **7**, 204.

29 M. Bajpai, K. Kumari, R. Srivastava, M. N. Kamalasanan, R. S. Tiwari and S. Chand, *Solid State Commun.*, 2010, **150**, 581.

30 J. H. Burroughes, D. D. C. Bradley, A. R. Brown, R. N. Marks, K. Mackay, R. H. Friend, P. L. Burns and A. B. Holmes, *Nature*, 1990, **347**, 539.

31 J. S. Kim, R. H. Friend, I. Grizzi and J. H. Burroughes, *Appl. Phys. Lett.*, 2005, **87**, 023506.

32 K.-H. Yim, G. L. Whiting, C. E. Murphy, J. J. M. Halls, J. H. Burroughes, R. H. Friend and J.-S. Kim, *Adv. Mater.*, 2008, **20**, 3319.

33 C. Tanase, E. J. Meijer, P. W. M. Blom and D. M. de Leeuw, *Phys. Rev. Lett.*, 2003, **91**, 216601.

34 C. Tanase, P. W. M. Blom and D. M. de Leeuw, *Phys. Rev. B: Condens. Matter Mater. Phys.*, 2004, **70**, 193202.

35 P. Tyagi, R. Srivastava, A. Kumar, S. Tuli and M. N. Kamalasanan, *Org. Electron.*, 2013, **14**, 1391.

36 I. Katsouras, A. Najafi, K. Asadi, A. J. Kronemeijer, A. J. Oostra, J. A. Koster, D. M. de Leeuw and P. W. M. Blom, *Org. Electron.*, 2013, **14**, 1591.